

MICROWAVE SIGNATURE OF POLAR FIRN AND SEA ICE IN THE ANTARCTIC FROM AIRBORNE OBSERVATION

Takashi YAMANOUCHI and Makoto WADA

National Institute of Polar Research, 9–10, Kaga 1-chome, Itabashi-ku, Tokyo 173

Abstract: Airborne observations of 19.35 GHz microwave radiation were taken over the sea ice and firn cover of Antarctic ice sheet. Microwave brightness temperature was analyzed to explain satellite observations.

As for the polar firn over the ice sheet, brightness temperature varied greatly from the coast to the interior, which noticeably corresponded to the mean annual accumulation obtained at the surface. Also found was the variation of brightness temperature on a small scale of about 1–10 km, which became extreme in the sastrugi/glazed surface zone (Z route), where the accumulation is variable. Calculated emissivity using the semi-empirical relation to the accumulation rate and physical temperature proposed in the past could not always explain the observed emissivity because of the limit of the theoretical relation, or shortage of measurements. Satellite passive microwave observations were of very low resolution, making it difficult to show these small scale great variations corresponding to the surface accumulation.

In the sea ice area, the brightness temperatures observed were similar to the results from the satellite. Brightness temperature was low for multi-year ice and high for first year fast ice; the brightness temperature for new ice increases from a lower value and converges to the value of first year ice.

From the flight across Riiser-Larsen Peninsula, smooth variation up to 225 K was seen over the central part of the peninsula. This high value could be explained by the extremely high accumulation, which occurred asymmetrically against the height of the peninsula. Also along the flight, it was easy to distinguish the ice shelf and sea ice, even when covered with snow, by microwave brightness temperature measurement.

1. Introduction

Recently, microwave observations from satellites have revealed sea ice extent and concentration, and accumulation rate of polar firn over the ice sheet and glacier (ZWALLY and GLOERSEN, 1977). Microwave radiation has an advantage over visible and infrared radiation in its ability to sense snow and ice surface conditions up to some depth, even under clouds. Remote sensing of surface condition of the polar cryosphere is an urgent need for the global change issue. Extensive Antarctic sea ice data were presented from Nimbus 5 ESMR by ZWALLY *et al.* (1983), showing the variation of sea ice extent and ice concentration. Many studies have been continued till today to clarify the relation of multi-frequency microwave data to the sea ice condition (*e.g.*, COMISO and SULLIVAN, 1986; COMISO *et al.*, 1989). As for the polar firn, several works have

been done to explain the microwave brightness temperature of satellite observation by the accumulation rate through snow particle size (CHANG *et al.*, 1976; ZWALLY, 1977). The relation of microwave data to the physical characteristics of the surface is still uncertain and many ground-truth works have been conducted. However, it is still difficult to explain the microwave properties only from simple physical parameters.

This paper, aiming to interpolate ground-truth and satellite observations, describes airborne microwave observations of intermediate scale. Airborne microwave observations had already been conducted more than 20 years ago to propose and evaluate the satellite observations (WILHEIT *et al.*, 1972; GLOERSEN *et al.*, 1973). We have also carried out airborne microwave observations over the seasonal snow cover over Japan Island in 1981–83 (WADA *et al.*, 1982; KUSUNOKI, 1984). However, no airborne microwave observations have been made on the Antarctic ice sheet.

2. Observations

Airborne microwave observations were made by the 28th Japanese Antarctic Research Expedition (JARE) using a Pilatus Porter PC-6 airplane in 1987. A 19.35 GHz radiometer (Shimada Rika Inc.) was used for the microwave measurements (KUSUNOKI, 1984). The radiometer antenna is 50 cm in diameter, has gain of 33 db, and is equipped with a radome. The receiver is of Dicke type, 100 MHz band width and linear polarization. Calibration was done at liquid nitrogen (air) temperature. A microwave radiometer parabolic antenna was installed in the floor of the airplane, looking toward the nadir as shown in Fig. 1. An infrared radiation thermometer (Barnes, PT-5) to measure the surface temperature, 35 mm still camera to monitor the surface and thermometer to monitor the antenna physical temperature were also installed in the floor. Amplifier and recording instruments were set on the rack (Fig. 1). Data were recorded every 1 s on cassette magnetic tape (CMT), were printed out every 10 s. These were used in the present analysis. Analogue data were also recorded. Since the airplane speed

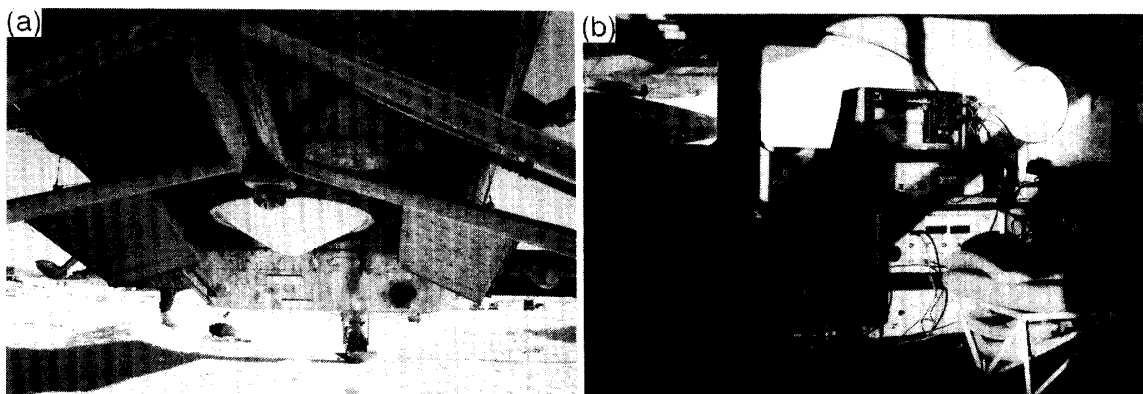


Fig. 1. (a) Microwave radiometer installed in the floor of Pilatus Porter plane together with precision infrared radiometer (PIR) and holes for the infrared radiation thermometer and 35 mm camera. (b) Amplifier, controller and recording instruments set on a rack inside the plane.

was approximately 180 km/h, abscissas of those figures showing flight records are expressed in distance (km) and data of every 10 s are plotted at every 0.5 km. Since the flight was at 600 to 900 m height, the instantaneous field of view was about 30 to 50 m corresponding to the 3° beam width of the antenna.

The brightness temperature T_B is derived as follows (WADA, 1991). From the output voltage V of the microwave radiometer, the antenna temperature T_1 is calculated as

$$T_1 = aV + b, \quad (1)$$

where a and b are calibrated constants related to the radiometer characteristics. Since the radiometer's antenna has considerable antenna loss L_A , the brightness temperature T_B is related to antenna temperature T_1 through antenna physical temperature T_A by

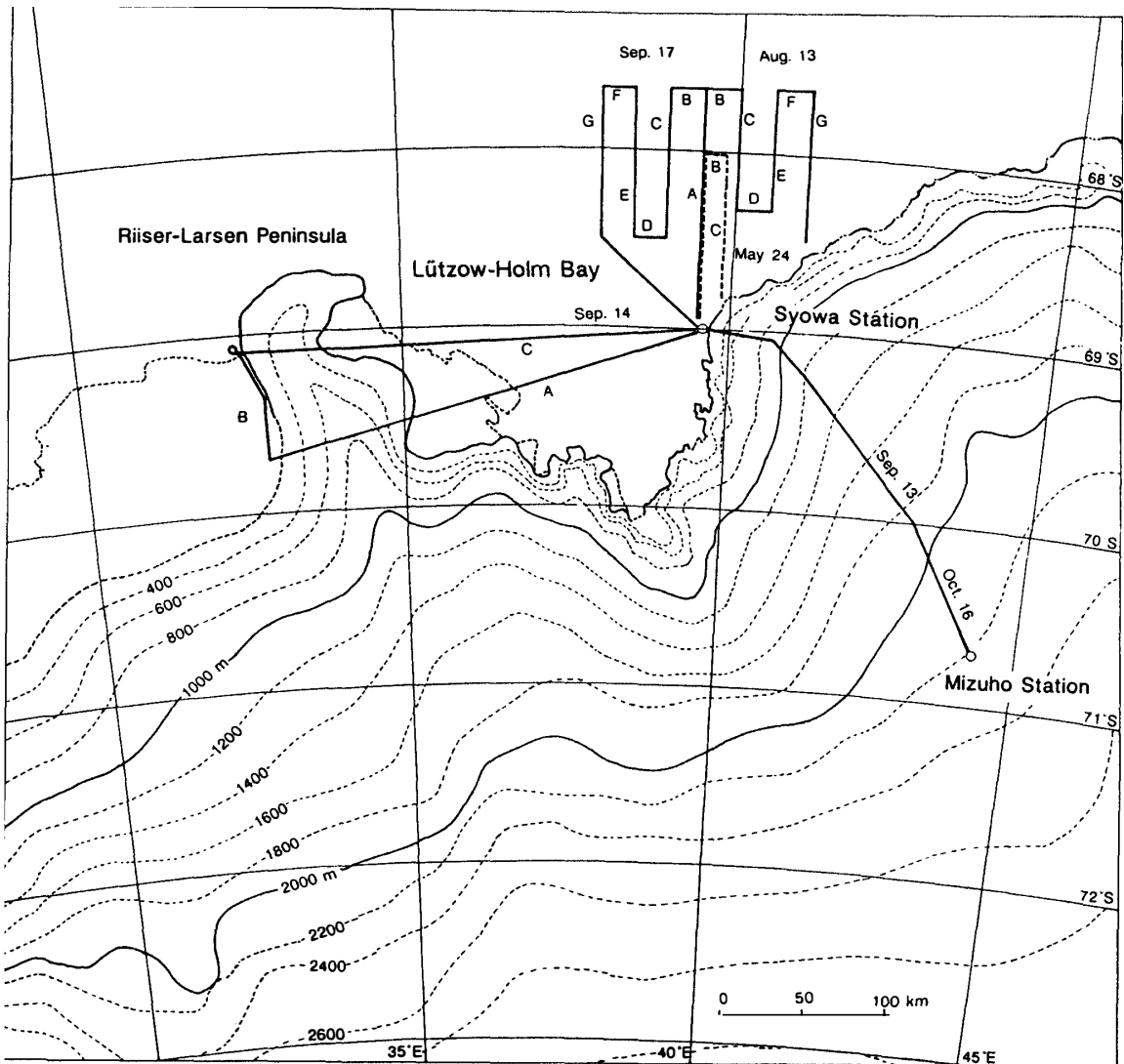


Fig. 2. Flight routes for airborne microwave observations referred to in the present paper. Dates shown along the route are dates of flights, and initials, A, B, ... are name for each leg within each flight.

$$T_I = (1 - L_A) T_B + L_A \cdot T_A \quad (2)$$

The value of L_A was determined in the course of surface observation of atmospheric water vapor and liquid water content in 1988, compared to the estimated water vapor amount from aerological observations (WADA, 1991). Figure 2 shows the flight route and dates of flights.

3. Polar Firn over Ice Sheet

3.1. Measured results

Two flights were made over the Mizuho Plateau, along the traverse routes between Syowa and Mizuho Stations, on September 13 and October 16, 1987. Figure 3 shows the microwave brightness temperature and infrared brightness (surface) temperature on October 16 on the way back from Mizuho to Syowa Stations. The microwave brightness temperature shows a large scale, about 50 km, and very noticeable variation on average. Starting from Syowa Station, after the high T_B of sea ice, quite low T_B around 170 K occurred. Then there appeared high T_B of about 200 K, where the altitude is between 600 and 1300 m, which roughly corresponds to the "S route". There appeared a rather smooth

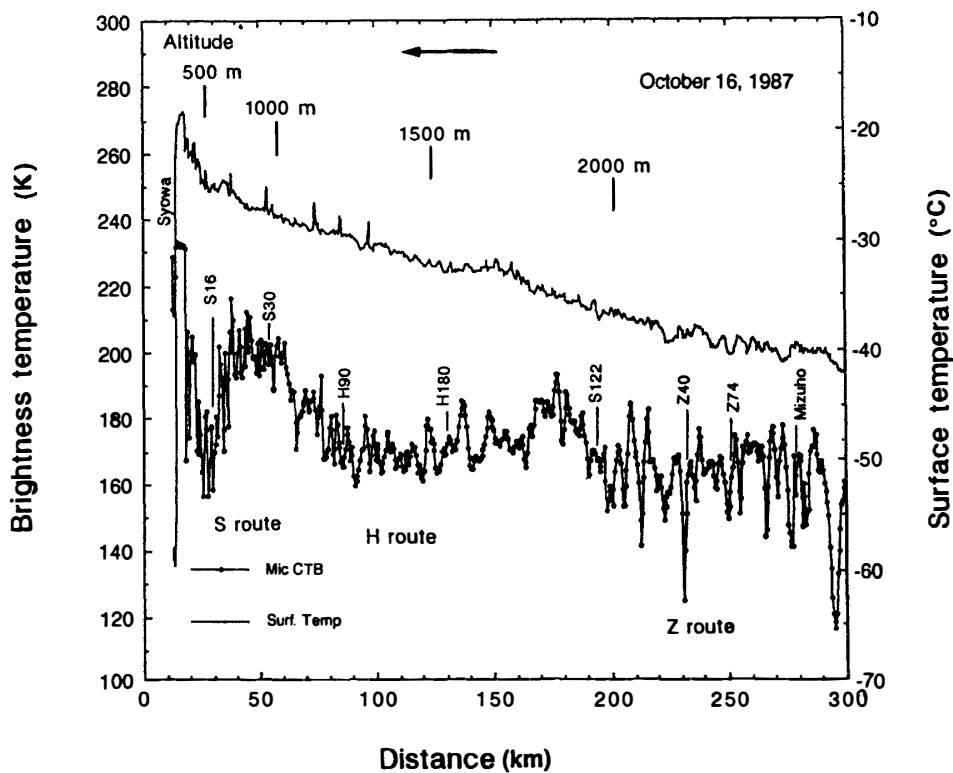


Fig. 3. 19.35 GHz microwave brightness temperature and surface temperature by infrared radiation thermometer from airborne observation, along the traverse route from Mizuho to Syowa Stations, October 16, 1987. Numbers in the figure show flag numbers along S, H, and Z routes, horizontal arrows show the flight direction.

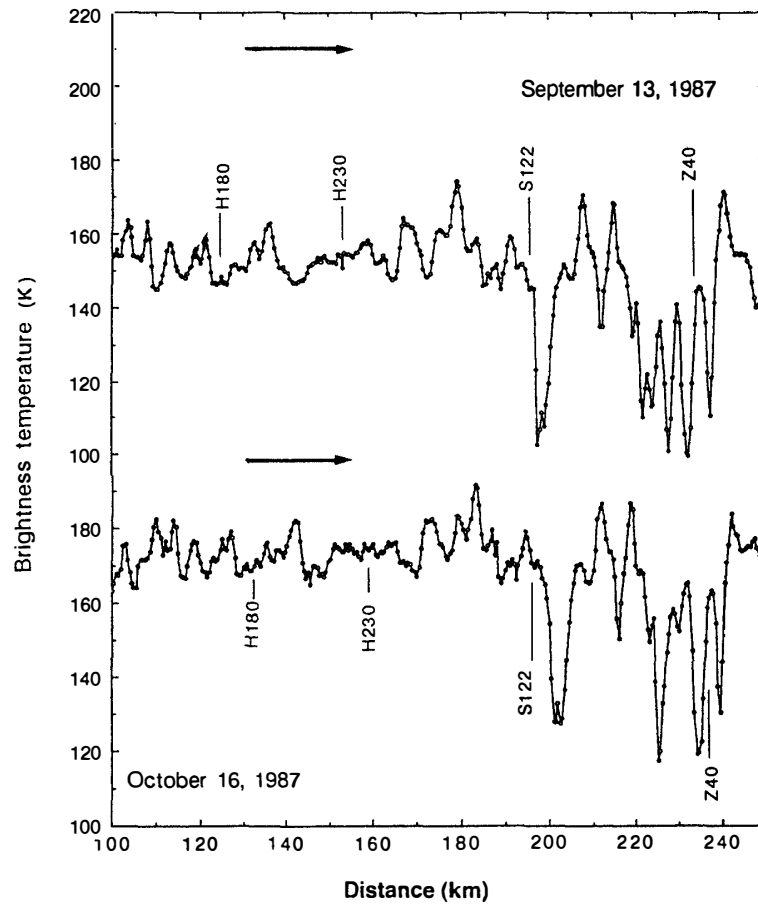


Fig. 4. Comparison of the brightness temperature from airborne observation along the traverse route from Syowa to Mizuho Stations on two days, September 13 and October 16, 1987.

curve of T_B around 170 K, where the altitude ranges from 1300 to 1800 m, roughly corresponding to the “H route”. Lastly, T_B was around 160 to 170 K, with extremely large variations on a small scale, in the altitude range from 1900 m, corresponding roughly to the “Z route”. Observations of the microwave brightness temperature on the way from Syowa to Mizuho Stations on September 13 and October 16 were also made. Large scale variations similar to Fig. 3 were seen in both flights.

There are also frequent oscillations in the brightness temperature less than 10 km in scale, and sometimes larger than 20 K in amplitude. These variations are neither random nor periodic, but have some physical meaning. The same variation pattern as on September 13 reappeared on October 16. Figure 4, enlarged, shows excellent correspondence between two data sets even one month apart, from flights in the same heading direction, but the air temperature was about 20° different.

3.2. Accumulation rate

Large scale variation in the microwave brightness temperature as shown in Fig. 3 was found to resemble the 1987 annual accumulation curve, shown in Fig. 5 by ZHANG and YAMANOUCHI (1991). This annual accumulation had been measured on the surface by a simple stake method (SATOW, 1985). Since the microwave measurements were done over the continental ice sheet, the correlation to the accumulation rate raises possibilities for the microwave brightness temperature to be affected by the accumulation rate through some surface conditions or physical properties of snow. Annual accumulations of other years are also examined (AGETA *et al.*, 1987; FUJII *et al.*, 1986; NAKAWO *et al.*, 1984; NISHIO and OHMAE, 1989; NISHIO *et al.*, 1988). The 5-year mean from 1983 to 1987, shown in Fig. 5, correlates highly to the brightness temperature/emissivity of October 16 (Fig. 3). The relation is shown in Fig. 6, where the emissivity ϵ was derived simply as a ratio of single measured T_B against surface temperature obtained by infrared radiation thermometer. The best fit line of annual accumulation A_a (cm/a) shown in the figure is expressed as

$$\epsilon_S = \frac{T_B}{T_S} = 0.68 + 0.0014A_a. \quad (3)$$

Relations among the large scale representative values are shown in Table 1. In the table, T_{10} is the 10 m depth temperature, which indicates approximately the annual average temperature, and $\epsilon_S = T_B / T_S$, $\epsilon_{10} = T_B / T_{10}$. These large variations in the brightness temperature/emissivity are related to the snow surface features of the ice sheet on Mizuho Plateau as described by WATANABE (1978) and to the surface accumulation characteristics expressed by SATOW (1985). High brightness temperature T_B around the S route corresponds to the high

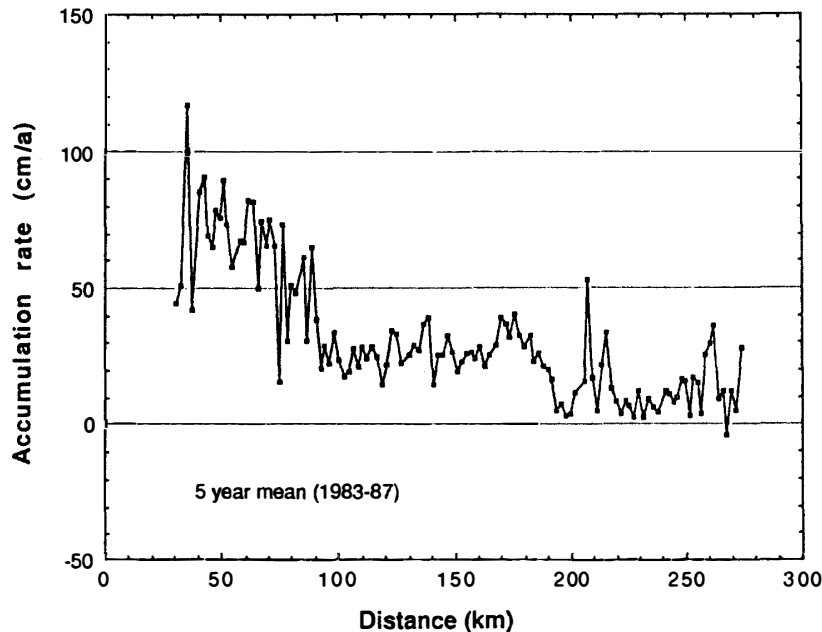


Fig. 5. 5-year mean (1983-1987) of annual accumulation along the traverse route between Syowa and Mizuho Stations.

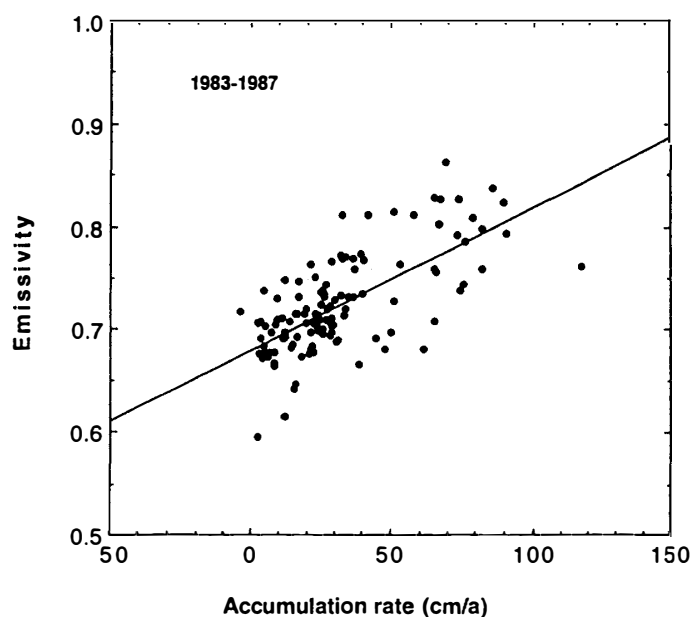


Fig. 6. Relation between annual accumulation (5-year mean) and emissivity of 19.35 GHz microwave radiation along the traverse route between Syowa and Mizuho Stations, October 16, return flight (Fig. 3).

Table 1. Microwave brightness temperature, emissivity and 5 year mean (1983-87) accumulation rate in three representative areas along the routes between Syowa and Mizuho Stations.

Region	Accumulation rate	T_B	ϵ_S	T_{10}	ϵ_{10}
S route (S16-H60)	72 cm/a 31 g/cm ² /a	192 K	0.78	253 K	0.76
H route (H60-S122)	31 13	173	0.72	248	0.70
Z route (S122-Z102)	13 5.5	162	0.69	243	0.67

* $\epsilon_S = T_B / T_S$, $\epsilon_{10} = T_B / T_{10}$.

accumulation rate near the coast, higher in altitude than the firn line about 600 m. Medium T_B around the H route corresponds to an amount of the accumulation smaller than on the S route, but larger than on the Z route. Lower T_B around the Z route corresponds to the low accumulation rate. Another low brightness temperature at the coast corresponds to the ablation zone, lower in altitude than the firn line. The surface snow in the ablation zone was interpreted by ZWALLY and GLOERSEN (1977) and ZWALLY (1984) as meaning that the snow would melt in summertime, when the brightness temperature become extremely high, and become blue ice and percolation ice, showing low emissivity/brightness temperature in the non-melting season. These airborne measurements were only made during the non-melting season, and showed low brightness temperature.

It is surprising that some part of small scale frequent variations of the brightness temperature are also correlated to the accumulation curve in Fig. 6. These small scale variations are much pronounced on the Z route of the sastrugi/glazed surface zone, where the accumulation does not continue smoothly, but occurs intermittently (FUJII, 1981), and variations are small on the H route of the smooth surface zone, where steady continuous accumulation occurs. These circumstances mean that variations depend on the accumulation process, which determines the properties of the firn layer. Since the optical depth of dry snow/firn is on the order of 5 m (ZWALLY, 1977), it is reasonable that the brightness temperature variation depends not on the real surface condition as seen in AVHRR visible or infrared imagery (FUJII *et al.*, 1987; FURUKAWA *et al.*, 1991), but on the thick layer accumulated during more than 5 or 10 years.

3.3. Model calculation

Attempts have been made to explain the microwave brightness temperature/emissivity of firn or snow by a theoretical radiative transfer model. CHANG *et al.* (1976) obtained a qualitative explanation of the low brightness temperature of the polar firn. ZWALLY (1977) has solved the radiative transfer equation with depth dependent parameters and through several approximations, including the neglect of multiple scattering, obtained an analytic expression. The results of these models show the dependence of microwave emissivity on snow particle size and physical temperature distribution. If we suppose the dry polar firn to be composed of small ice particles, microwave radiation at the surface is a summation of the radiation emitted from some thick layer. So the physical temperature distribution has the meaning and the particle size distribution determines the scattering which controls the emissivity. On the other hand, accumulation rate and physical temperature are known to control the snow particle size. COMISO *et al.* (1982) also calculated the radiation transfer equation with depth-dependent parameters without neglecting multiple scattering, and reached to better agreement with observations including seasonal variation. Though different in approximation level, none of them could completely explain the observed values. ROTMAN *et al.* (1982) made an empirical fitting, using the equation derived by ZWALLY (1977) using an accumulation rate A and 10 m temperature T_{10} with two empirical fitting parameters, determined by comparing the microwave emissivity by Nimbus 6 SCAMS to the accumulation rate data obtained as a climatological value estimated over the Antarctic continent based on some point measurement at the surface.

Following Rotman's empirical fitting, emissivity was calculated with empirical parameters extrapolated to 19.35 GHz from values at 22 and 31 GHz. Calculated results for $T_{10}=213, 243, 248$ and 253 K are shown in Fig. 7; the latter three correspond to the measured points of Table 1, also plotted in the figure. Solid circles are the emissivities derived as the ratio of T_B to the infrared surface temperature T_S ; white circles are emissivities calculated as the ratio of T_B to the annual mean temperature T_{10} . In Fig. 7, only the accumulation rate plot from the route H lies near the calculated curve. The other two points diverge from the

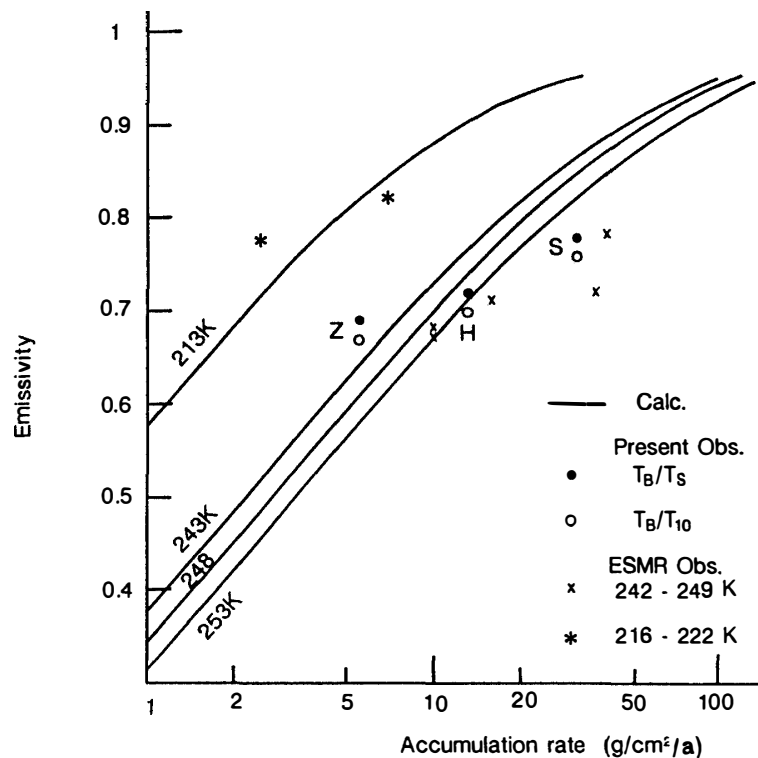


Fig. 7. Relation between accumulation rate and 19.35 GHz microwave emissivity of semiempirical calculation derived from ROTMAN *et al.* (1982) based on ZWALLY (1977), and compared are the large scale mean of airborne observation for S, H and Z routes (Table 1). Solid circles are the emissivities derived as ratios of T_B to the infrared surface temperature T_S and white circles are emissivities as ratios of T_B to the annual mean temperature T_{10} . Also compared are the satellite observations of Nimbus 5 ESMR, referred to by COMISO *et al.* (1982) and ZWALLY (1977) at several stations where the firn properties are known.

calculated curves. Plots from airborne observation suggest much larger dependence of the modeled emissivity to the physical temperature and smaller dependence on the accumulation rate. The empirical fitting by Rotman cannot always explain the observed values. Observed values are also liable to have some ambiguity owing to some bias error similar as discussed by YAMANOUCHI *et al.* (1992), problems in derivation of emissivity (calibration of brightness temperature, physical temperature distribution, etc...) and also problems in the accumulation rate measurement data. In Fig. 7, also plotted are observed emissivities by Nimbus 5 ESMR at some particular points (different from the present study area) where the accumulation rate had been measured, referred to by ZWALLY (1977) and COMISO *et al.* (1982). These ESMR emissivities seem to have rather similar dependence on the accumulation rate and temperature as the present observations. These results indicate that the theory can generally explain the observations, but cannot follow the individual dependence.

3.4. Comparison with satellite observation

As the final objective, airborne microwave observation was compared with satellite observations. One series is Microwave Scanning Radiometer (MSR) data of MOS-1, which are composed of two channels 23.8 and 31.4 GHz (YAMANOUCHI *et al.*, 1991). Since the nominal fields of view for these channels are 31 and 23 km, the data of high resolution channel 31.4 GHz are compared. Brightness temperatures at 31.4 GHz from MOS-1 MSR, along the traverse route between Syowa and Mizuho Stations, from the data of path 57 in the same season (September) as airborne observation, are shown in Fig. 8, together with a summer example (February). Compared to Fig. 3, these MSR values can show neither variations smaller in scale than the field of view of 20 km, nor larger smooth variations of about 50 km scale. This is owing not only to the effect of the antenna side lobe but also to the data resampling, which includes some averaging effect. However, though different in frequency and the year, MSR brightness temperatures in September roughly indicate large mean airborne observation values. After the monotonous decrease from Syowa to Mizuho Stations, there seems to be a small increase again from Mizuho Station. This reversal may correspond to the increase of accumulation rate inland from Mizuho Station, mentioned by TAKAHASHI and AGETA (1991). It is possible to evaluate large scale mean accumulation rate (KOIKE *et al.*, 1991). However, an ablation zone or high accumulation zone as discussed in the previous section is hard to be detected by MSR observation.

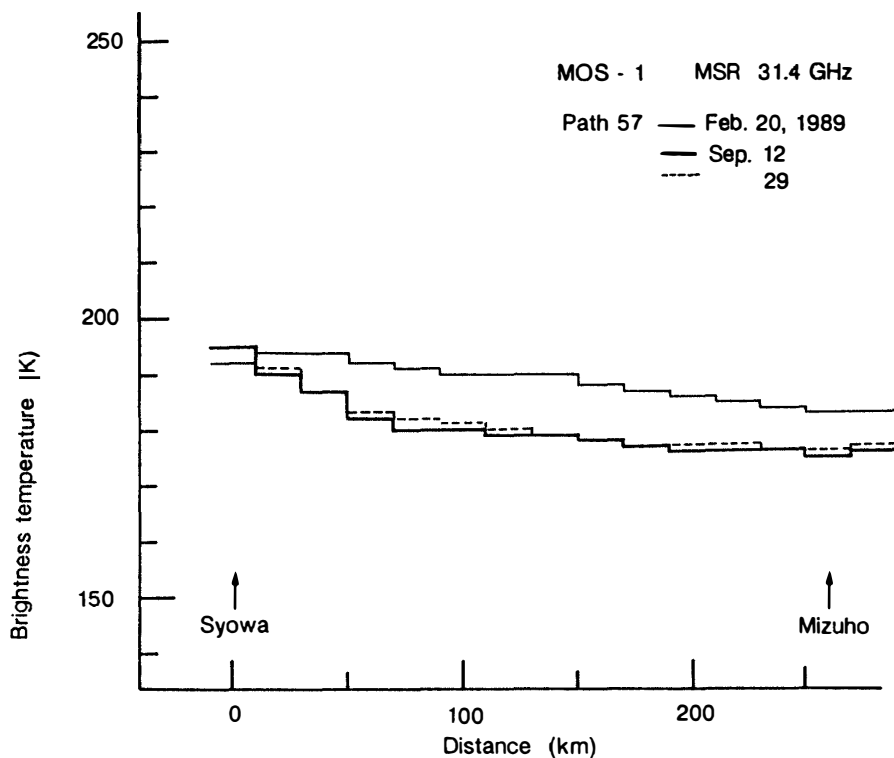


Fig. 8. MOS-1 MSR 31.4 GHz brightness temperature along the route between Syowa and Mizuho Stations from path 57, on February 20, September 12 and 29, 1989.

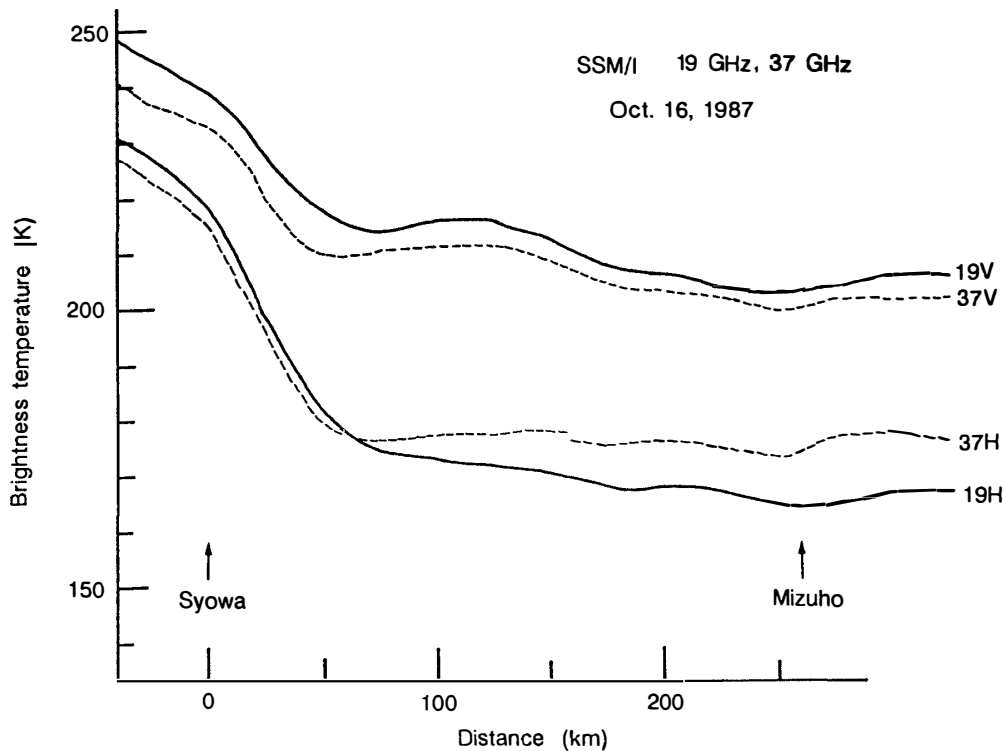


Fig. 9. SSM/I 19 and 37 GHz brightness temperatures along the route between Syowa and Mizuho Stations from the gridded data of October 16, 1987. V denotes vertical and H denotes horizontal polarization.

It is also interesting to know the brightness temperatures by SSM/I of the DMSP satellite (HOLLINGER *et al.*, 1990), which are widely used. Figure 9 shows the variation of 19 and 37 GHz brightness temperatures obtained by vertical and horizontal polarization from the grid point near the route between Syowa and Mizuho Stations, as in Fig. 8. The data are from the same date as one of the airborne observations, October 16, 1987. Though the effective fields of view are 55 and 33 km for 19 and 37 GHz, respectively, Fig. 9 shows much higher resolution than Fig. 8; however, one still cannot follow 20 to 30 km variations as shown in Figs. 3 or 4, and it is difficult to find an ablation zone or high accumulation zone near the coast. Because of the high brightness temperature of sea ice off the coast, it is difficult to separate the effects of sea ice and ice sheet surface and to assign the coast line.

4. Flight over Sea Ice

Figures 10 to 12 show data from flights over the sea ice area on May 24, August 13 and September 17, 1987. Each flight passes over fast ice from Syowa Station to the edge of the fast ice where the flaw lead (called "Ôtone Lead") lies as shown in Fig. 2, and then over the pack ice area including open water. On the flight routes near Syowa Station, there appeared a variable microwave brightness temperature, caused by first year ice or new ice formed since the

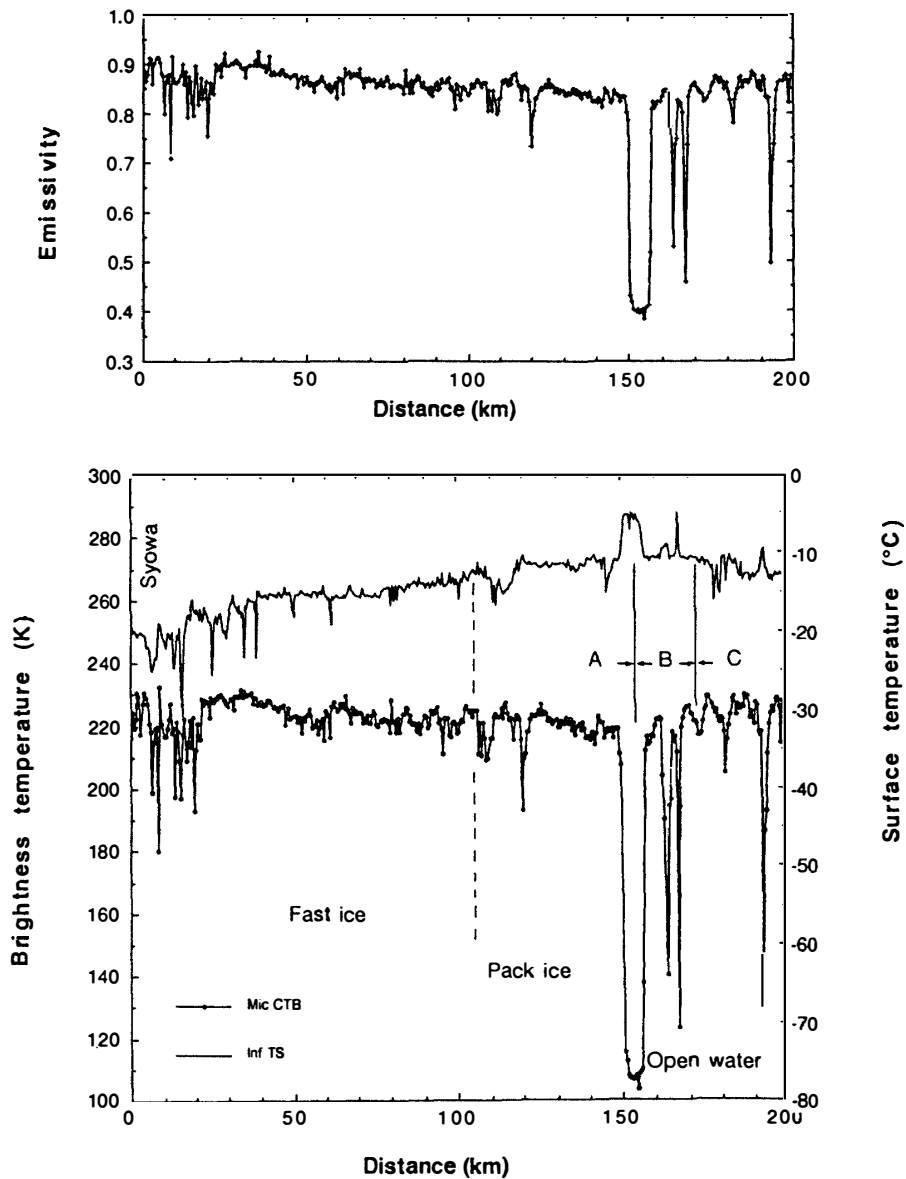


Fig. 10. 19.35 GHz microwave brightness temperature, surface temperature by infrared radiation thermometer, and emissivity as the ratio from airborne observations along the route from Syowa Station over the sea ice area, May 24, 1987.

outflow of sea ice in March, April and June off the west coast of the Ongul Islands. Then appeared a rather low brightness temperature between 210 and 220 K, indicating multi-year sea ice, which lasted for years during the sea ice outflow season near Ongul Islands. Some spike-like noise in this area corresponds to lower infrared surface temperature, owing to icebergs which have lower emissivity. In Figs. 11 and 12, most of the surface between coastal multi-year sea ice and Ôtone Lead is covered with very smooth first year ice, which has only a few degrees variation. At the edge of the fast ice, there lies a flaw lead, one kind of coastal polynya, Ôtone. From this edge, there is a pack ice area, mixture of ice

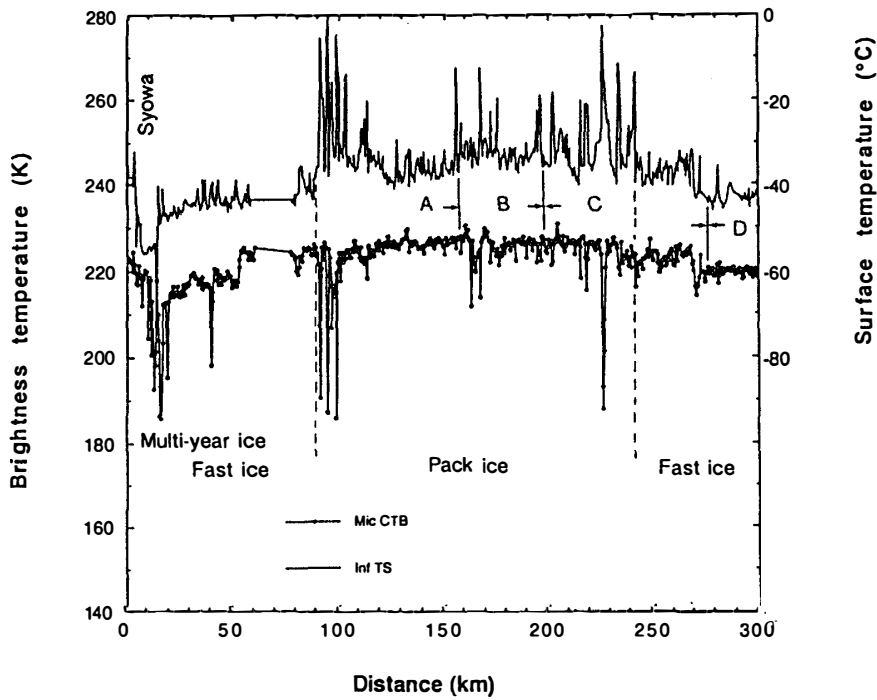


Fig. 11. 19.35 GHz microwave brightness temperature and surface temperature by infrared radiation thermometer from airborne observations along the route from Syowa Station over the sea ice area, August 13, 1987.

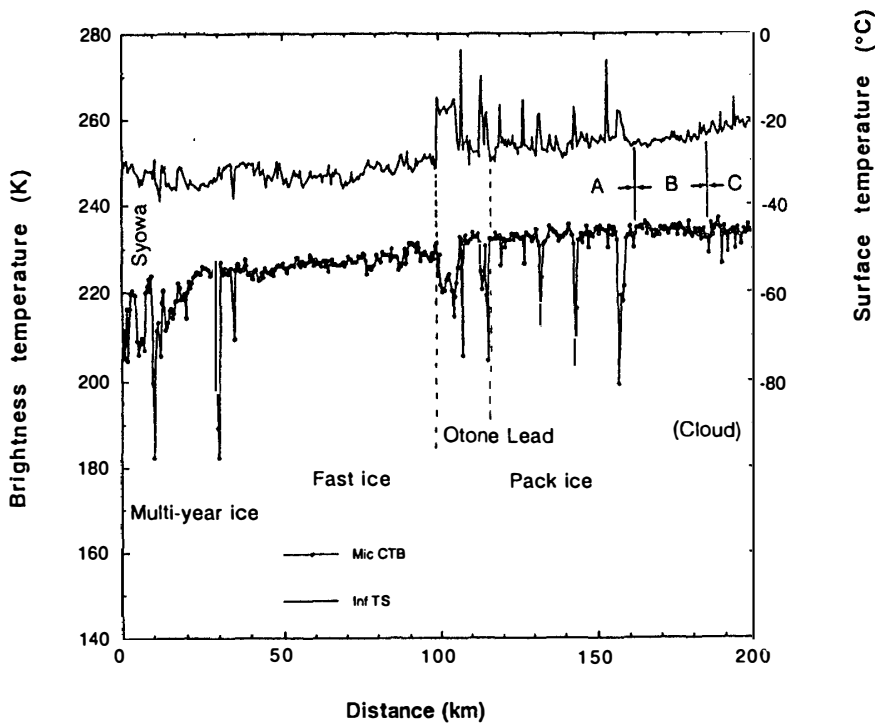


Fig. 12. Same as Fig. 12 but for September 17, 1987.

floes and open water. In this case, a lower spike in the microwave brightness temperature corresponds to a higher spike in the surface temperature, indicating melting ice surface or open water.

Interesting is the gradual variation of the temperature from multi-year ice near Syowa Station to the pack ice area through first year fast ice. The brightness temperature in Fig. 10 for May 24 gradually decreases in this section, and the emissivity decreases much more steeply owing to the increase of surface temperature. On the other hand on August 13 and September 17 as shown in Fig. 11 and 12, though the emissivity gradually decreases from first year fast ice to the pack ice area, owing to the increase of surface temperature, the brightness temperature itself does not decrease but increases in the same leg. This is because the emissivity variation decreases according to the season from the first year fast ice near the coast to the new ice near the edge of fast ice, and then to the ice in the pack ice area. The emissivity of new ice is originally small; it increases with time and lastly converges to the value of first year ice (COMISO *et al.*, 1989). The lower emissivity of multi-year ice near Syowa Station is clearly seen in Fig. 11 or 12; however it is not clear in Fig. 10, maybe due to the difference in flight course.

Wide open water is seen in Fig. 10 at 150 km distance. The low microwave brightness temperature of about 105 to 110 K appears within 10 km width, where the infrared brightness temperature is about -5°C . There are also many other open water leads, seen in Figs. 10, 11 and 12; however, the microwave brightness temperature does not reach the true value for open water owing to the narrow width compared to the field of view of the microwave radiometer. The brightness temperature/emissivity of open water seems to be too low compared to the emissivity of 0.46 found by COMISO *et al.* (1989) or brightness temperature 120 K of ZWALLY and GLOERSEN (1977). A claim of absolute accuracy is not warranted, because, as explained in Section 2, the antenna loss L_A in eq. (2) was only determined afterward for atmospheric water vapor observation in the open air and might be different in airborne observation, also, T_S from the infrared radiation thermometer operated in low temperatures of about -20°C is not calibrated value. These values should rather be corrected using this open water measurement.

5. Flight Crossing Riiser-Larsen Peninsula

One flight crossing Riiser-Larsen Peninsula was conducted, since this course included interesting features of the surface temperature seen in the satellite infrared image. Figure 13 is one example of NOAA AVHRR data on September 13, one day before the flight. Quite low temperature were found on the shelf, western side of the peninsula and sea ice in Lützow-Holm Bay on the eastern side of the peninsula. On the other hand, both side slopes of the peninsula show higher temperatures in spite of their heights.

Figures 14 and 15 show the results for the flight. The results over the sea ice, 80 km from Syowa Station in Fig. 14 and 100 km in Fig. 15, are similar to

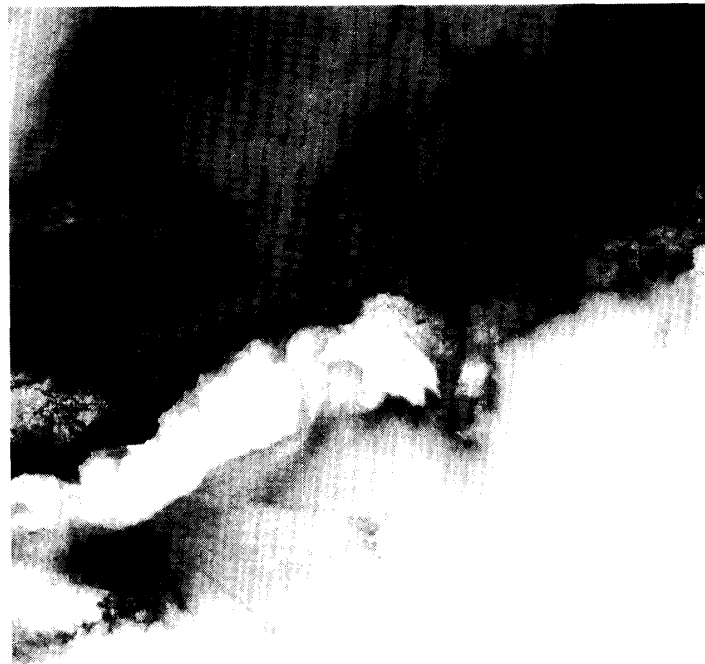


Fig. 13. NOAA AVHRR infrared (channel 4 and 5) image around Riiser-Larsen Peninsula and Lützow-Holm Bay, September 13, 1987.

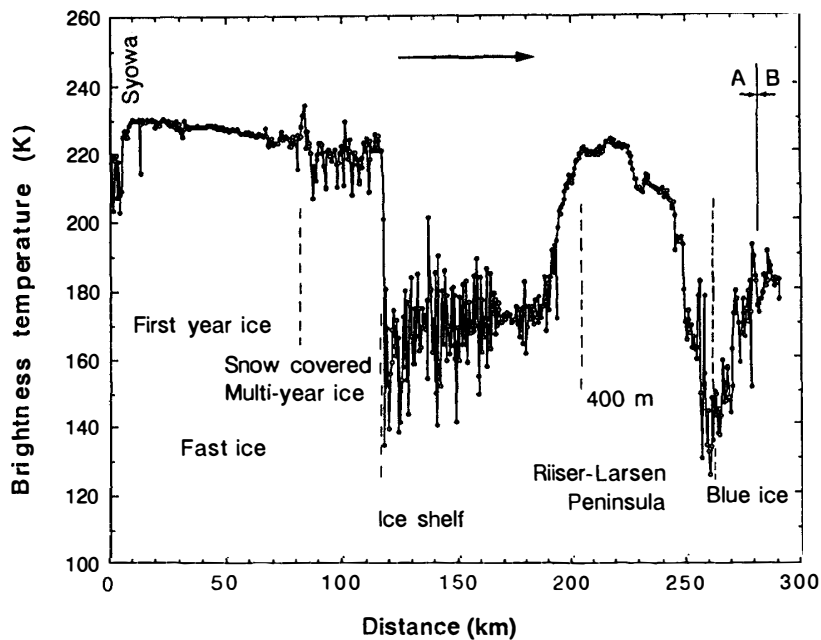


Fig. 14. 19.35 GHz microwave brightness temperature from airborne observation along the route from Syowa Station over the sea ice area and crossing Riiser-Larsen Peninsula, September 14, 1987.

those explained in the last section. The new ice produced in the middle eastern part of the bay at 30 to 50 km distance has low brightness temperature with a slightly higher surface temperature, as seen in Fig. 15. Sea ice in the western half of the bay shows a much lower surface temperature, as seen in Fig. 15 and also

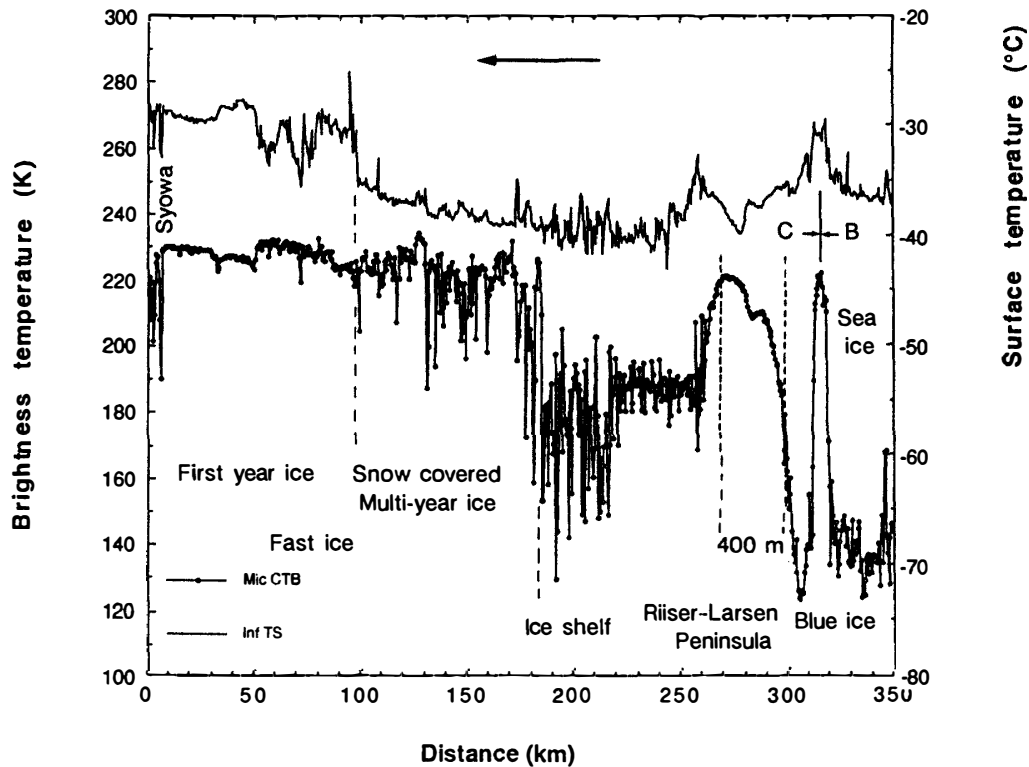


Fig. 15. 19.35 GHz microwave brightness temperature and surface temperature by infrared radiation thermometer from airborne observation along the route crossing Riiser-Larsen Peninsula, over the sea ice area to Syowa Station, return flight of the route shown in Fig. 14, September 14, 1987.

in the AVHRR image of Fig. 13; however, the decrease in the microwave brightness temperature is not so large although the variation becomes large. The sea ice in this area did not flow out through out the year and is of multi-year ice (YOSHIDA and MORIWAKI, 1990). The reason of high emissivity for this area is due to the lower surface temperature of the thick snow cover on the ice surface (TAKIZAWA, private communication). Owing to the effect of thick snow as an insulator, the real ice surface is not so cooled and the meaningful emissivity of multi-year ice might be much lower, as explained in Fig. 2 of COMISO *et al.* (1989). The situation is not noticeable in Figs. 10 to 12, because the snow thickness is much smaller on the eastern side of Lützow-Holm Bay.

Large gaps in the microwave brightness temperature are seen around 115 and 180 km in Figs. 14 and 15, respectively, where no noticeable change is seen in the surface temperature. The low brightness temperature around 180 K is due to land ice (firn/snow) as already seen in Section 3. Since the surface is covered with thick snow, it is difficult to distinguish between sea ice and land ice visually, or by infrared surface temperature; however, both are clearly distinguished by the microwave. Within similar average brightness temperature, there are two variations. One part near the sea ice between the 115 and 150 km or between the 180 and 220 km points in Figs. 14 and 15, respectively, made of floating land ice tongue and ice shelf shows very large variance, maybe partly due to cracks

between ice floes. Another part near the slope of peninsula shows smaller variance, maybe due to the smoother surface of the ice shelf; however, the actual difference is not clear.

The most striking feature in Figs. 14 and 15 is the smooth mountain-like feature up to 220 K in the microwave brightness temperature over the main part of the peninsula from 190 to 240 or from 260 to 300 km distance in Figs. 14 and 15, respectively. 190 or 260 km distance corresponds to an altitude of about 100 m. Compared to the flight route shown in Fig. 2 or to the surface temperature in Fig. 15, the summit of the peninsula, about 750 m for the route shown in Fig. 14 and about 550 m for the route in Fig. 15, is located around the small dip in the mountain-like curve, at the 230 km and 280 km points, respectively, for Figs. 14 and 15. So the brightness temperature curves are not symmetrical with respect to the summit, but are higher on the east side slope and lower on the west side slope. We have no certain evidence to explain this striking feature because there are no ground truth measurements. The position of the summit itself is also not ascertained.

One possible explanation is an extremely high accumulation rate. The highest brightness temperature of the smooth curve, about 225 K, will result in the maximum emissivity about 0.95 and accumulation of about 2 m/a from Fig. 6. The recalculated emissivity of about 0.88 with T_{10} between -15 to -20°C , will yield an accumulation rate of about 60 to 70 $\text{g}/\text{cm}^2/\text{a}$, which means about 1.4 to 1.6 m in snow depth from the relation by ROTMAN *et al.* (1982) as in Fig. 7. This high accumulation rate will produce a smooth firn layer of a few meters thick during one year, and since the penetration depth of the 19 GHz microwave is about 5 m, as already discussed in Section 3, emitted microwave radiation will vary smoothly within the region of extremely high accumulation rate. The asymmetry of the brightness temperature curve is due to the asymmetry of the accumulation, depending on the asymmetry of precipitation or wind condition due to the difference in the slope direction. The slope facing the east has higher precipitation and the slope facing the west has lower precipitation, which can also be seen on the west faced slope of Mizuho Plateau. The extremely high precipitation might be caused by the topographical effect of the steep peninsula penetrating into ocean.

The surface temperature curve in Fig. 15 over the peninsula also shows an interesting feature. The surface temperature of the peninsula is shifted about 10°C higher as a whole compared to the flat sea level surfaces of the ice shelf and sea ice surrounding the peninsula. The highest surface temperature appears near the bottom of the slope where the downslope wind-katabatic wind-is strongest. Katabatic wind affects almost the whole area of peninsula, which makes the surface temperature higher by destroying the surface inversion and by adiabatic heating. The low surface temperature over the ice shelf is due to weak wind owing to the flat surface. The blue ice area is of high temperature owing to the low albedo of the surface.

The higher microwave brightness temperature around 220 K and the higher surface temperature at the 315 km point are caused by sea ice observed at the

corner of the flight route. The low temperature of 130 to 140 K around that point is due to the blue ice area–ablation zone–similar to the area already discussed for the Mizuho route in Section 3. The bottoms of the slopes on the eastern and western sides of the peninsula have different firn surface features as shown by the microwave brightness temperature. The blue ice is typical, and ablation is active on the west-facing slope, also similar to the Mizuho route. This phenomenon is also due to the difference in precipitation and wind condition depending on the slope direction.

6. Concluding Remarks

Airborne 19 GHz microwave observations revealed several interesting characteristics of the Antarctic snow and ice.

- 1) Microwave brightness temperature of the polar firn showed a good correlation with the annual accumulation measured at the surface. The high accumulation zone near the coast and low accumulation–ablation–zone could be nicely traced by the microwave brightness temperature/emissivity.
- 2) The distribution of microwave emissivity of the sea ice area was qualitatively similar to the results of satellite observations, lower emissivity for the multi-year ice and new ice, and higher emissivity for the first year ice. The emissivity of new ice increased to a higher value similar to first year ice, which meant that the ice was already not “new”.
- 3) Microwave brightness temperature along the route crossing the Riiser-Larsen Peninsula showed interesting features. Extremely high and smooth brightness temperatures appeared over the middle part of the peninsula, indicating an extremely high accumulation rate of about 1.5 to 2 m/a in snow depth. A noticeable gap in the microwave brightness temperature was found between multi-year sea ice and land ice; it was not detectable in the infrared brightness temperature or visible reflectance owing to the thick snow cover lying on the surface.

Since most of the features listed above are on small scale, 10 to 50 km, they were difficult to detect by satellite passive microwave observation. However, the monitoring of the high accumulation belt zone is indispensable for the study of mass balance and climate change research, so it is of great importance to continue such airborne microwave observations in the future.

Acknowledgments

The authors wish to express their sincere thanks to the members of JARE-28, led by Dr. Y. OHYAMA, National Institute of Polar Research, for their kind support of the flight operation. Special thanks are due to pilots M. MORI and K. OHMOTO, flight engineer F. ARUGA and support staff member K. MORIMOTO. This study would not have been realized without their vigorous efforts. The authors are much indebted to Mrs. N. KAGA for preparing the manuscript.

The observation was conducted under JARE-28 and analysis was supported financially in part by Grants-in-Aid for Scientific Research Nos. 02228225 and 03212106 from the Ministry of Education, Science and Culture of Japan.

References

- AGETA, Y., KIKUCHI, T., KAMIYAMA, K. and OKUHIRA, F. (1987): Glaciological Research Program in East Queen Maud Land, East Antarctica. Part 5, 1985. JARE Data Rep., **125** (Glaciology 14), 71 p.
- CHANG, T. C., GLOERSEN, P., SCHMUGGE, T., WILHEIT, T. T. and ZWALLY, H. J. (1976): Microwave emission from snow and glacier ice. *J. Glaciol.*, **16**, 23–39.
- COMISO, J. C. and SULLIVAN, C. W. (1986): Satellite microwave and *in situ* observation of the Weddell Sea ice cover and its marginal ice zone. *J. Geophys. Res.*, **91**, 9663–9681.
- COMISO, J. C., ZWALLY, H. J. and SABA, J. L. (1982): Radiative transfer modeling of microwave emission and dependence on firn properties. *Ann. Glaciol.*, **3**, 54–58.
- COMISO, J. C., GRENFELL, T. C., BELL, D. L., LANGE, M. A. and ACKLEY, S. F. (1989): Passive microwave *in situ* observations of winter Weddell Sea ice. *J. Geophys. Res.*, **94**, 10891–10905.
- FUJII, Y. (1981): Formation of surface snow layer at Mizuho Station, Antarctica. *Mem. Natl Inst. Polar Res.*, Spec. Issue, **19**, 280–296.
- FUJII, Y., KAWADA, K., YOSHIDA, M. and MATSUMOTO, S. (1986): Glaciological Research Program in East Queen Maud Land, East Antarctica. Part 4, 1984. JARE Data Rep., **116** (Glaciology 13), 70 p.
- FUJII, Y., YAMANOUCHI, T., SUZUKI, K. and TANAKA, S. (1987): Comparison of the surface conditions of the inland ice sheet, Dronning Maud Land, Antarctica, derived from NOAA AVHRR data with ground observation. *Ann. Glaciol.*, **9**, 1–4.
- FURUKAWA, T., SEKO, K., WATANABE, O. and WADA, M. (1991): Êsei gazô o mochiita Nankyoku hyôshô jôtai no bunrui-NOAA AVHRR gazô to DMSP ni yoru maikuro-ha gazô o riyô shite-(Surface conditions of the ice sheet, Antarctica, derived from NOAA AVHRR and microwave images). *Dai-14-kai Kyokuiki Kisuiken Shinpoijumu Puroguramu · Kôen Yôshi (Program · Abstract of the 14th Symposium on Polar Meteorology and Glaciology)*. Tokyo, Natl Inst. Polar Res., 45.
- GLOERSEN, P., NORDBERG, W., SCHMUGGE, T. J. and WILHEIT, T. T. (1973): Microwave signatures of first-year and multi year sea ice. *J. Geophys. Res.*, **78**, 3564–3572.
- HOLLINGER, J. P., PEIRCE, J. L. and POE, G. A. (1990): SSM/I instrument evaluation. *IEEE Trans. Geosci. Remote Sensing*, **28**, 781–790.
- KOIKE, T., SUHAMA, T., KOIKE, M. and YAMANOUCHI, T. (1991): Maikuro-ha rimôto senshingu ni yoru sekisetsu kansoku (Observation of snow by microwave remote sensing). *Dai-14-kai Kyokuiki Kisuiken Shinpoijumu Puroguramu · Kôen Yôshi (Program · Abstract of the 14th Symposium on Polar Meteorology and Glaciology)*. Tokyo, Natl Inst. Polar Res., 80–81.
- KUSUNOKI, K. (1984): Radiation and Microwave Studies of Cryosphere Surface for the Basis of Satellite Observations. Grant-in-Aid for Scientific Research, No. 56460038, 40 p.
- NAKAWO, M., NARITA, H. and ISOBE, (1984): Glaciological Research Program in East Queen Maud Land, East Antarctica. Part 2, 1983. JARE Data Rep., **96** (Glaciology 11), 80 p.
- NISHIO, F. and OHMAE, H. (1989): Glaciological Research Program in East Queen Maud Land, East Antarctica. Part 8, 1986–1987. JARE Data Rep., **148** (Glaciology 17), 59 p.
- NISHIO, F., OHMAE, H. and OSADA, K. (1988): Glaciological Research Program in East Queen Maud Land, East Antarctica. Part 7, 1986. JARE Data Rep., **143** (Glaciology 16), 49 p.
- ROTMAN, S. R., FISHER, A. D. and STAELIN, D. H. (1982): Inversion for physical characteristics of snow using passive radiometric observations *J. Glaciol.*, **28**, 179–185.
- SATOW, K. (1985): Variability of surface mass balance in the Mizuho Plateau, Antarctica. *Mem. Natl Inst. Polar Res.*, Spec. Issue, **39**, 134–140.

- TAKAHASHI, S. and AGETA, Y. (1991): Hyôshô no taiseiki kankyô (Accumulation feature of the Antarctic ice sheet). Nankyoku no Kagaku, 1. Sosetsu (Sciences in the Antarctic, 1. General Introduction), ed. by Natl Inst. Polar Res. Tokyo, Kokon Shoin, 65–85.
- WADA, M. (1991): Estimation of vertically integrated liquid water contents in the atmosphere. Nankyoku Shiryô (Antarct. Rec.), **35**, 1–11.
- WADA, M., YAMANOUCHI, T., KANZAWA, H., MAE, S., KAWAGUCHI, S. and KUSUNOKI, K. (1982): Maikuroha ni yoru sekisetsu no kansoku (Observation of snow by microwave radiometer). Nihon Seppyo Gakkai Shûki Taikai Kôen Yôshishû (Papers presented at the Annual Meeting of Jpn. Soc. Snow and Ice), 276
- WATANABE, O. (1978): Distribution of surface features of snow cover in Mizuho Plateau. Mem. Natl Inst. Polar Res., Spec. Issue, **7**, 44–62.
- WILHEIT, T., NORDBERG, W., BLINN, J., CAMPBELL, W. and EDGERTON, A. (1972): Aircraft measurements of microwave emission from arctic sea ice. Rem. Sensing Environ., **2**, 129–139.
- YAMANOUCHI, T., KANZAWA, H., ARIYOSHI, H. and EJIRI, M. (1991): Report on the first MOS-1 data received at Syowa Station, Antarctica. Proc. NIPR Symp. Polar Meteorol. Glaciol., **4**, 22–30.
- YAMANOUCHI, T., OSHIYAMA, T. and WADA, M. (1992): Analysis of MOS-1 MSR data received at Syowa Station, Antarctica. Proc. NIPR Symp. Polar Meteorol. Glaciol., **5**, 156–166.
- YOSHIDA, Y. and MORIWAKI, K. (1990): Some observations of sea ice in the vicinity of Lützow-Holm Bay, Antarctica. Nankyoku Shiryô (Antarctic Rec.), **34**, 8–14.
- ZHANG, W. and YAMANOUCHI, T. (1991): Surface mass balance and its variation on the Mizuho Plateau, Antarctica in 1987–1988. Antarct. Res., **2**, 10–21.
- ZWALLY, H. J. (1977): Microwave emissivity and accumulation rate of polar firn. J. Glaciol., **18**, 195–215.
- ZWALLY, H. J. (1984): Observing polar-ice variability. Ann. Glaciol., **5**, 191–197.
- ZWALLY, H. J. and GLOERSEN, P. (1977): Passive microwave images of the polar regions and research applications. Polar Rec., **18**, 431–450.
- ZWALLY, H. J., COMISO, J. C., PARKINSON, C. L., CAMPBELL, W. J., CARSEY, F. D. and GLOERSEN, P. (1983): Antarctic sea ice, 1973–1976: Satellite passive-microwave observations. NASA Spec. Publ., **459**, 206 p.

(Received December 27, 1991; Revised manuscript received May 22, 1992)